Dielectric properties of the hydrates of argon and nitrogen[1]

S. R. GOUGH, E. WHALLEY, AND D. W. DAVIDSON

Division of Applied Chemistry, National Research Council of Canada, Ottawa, Canada

Received December 5, 1967

The dielectric relaxation of water in the structure I clathrate hydrates of argon and nitrogen was studied over a range of temperature and pressure. Hydrates were slowly grown at pressures of 1 to 2 kbar in a coaxial cell enclosed in a pressure vessel. The complex permittivity loci resemble circular arcs with static dielectric constants of ~ 56 at 0 °C and high-frequency dielectric constants of 2.85 $\pm$ 0.05. Relaxation near 0 °C is about as slow as in ice I, but activation energies and entropies are much smaller. Formation of Bjerrum defects probably takes place preferentially near the occasional sites at which argon and nitrogen molecules have replaced water molecules in the lattice. The much faster relaxations found previously in the isostructural hydrates of ethers arise from orientational defects induced in the water lattice by the encaged molecules, a small proportion of which may form hydrogen bonds with water. The effect of small gaps in series with samples showing circular-arc dispersion behavior was evaluated.

Canadian Journal of Chemistry, **46**, 1673 (1968)

Dielectric relaxation associated with the reorientation of water molecules in ice (1, 2) and its high-pressure modifications (3, 4) has been previously studied. The gas, or clathrate, hydrates (5) are further examples of ices whose lattices consist of hydrogen-bonded four-coordinated water molecules. Stability is conferred upon these hydrates by the presence in the lattice cages of guest molecules, which typically seem to interact only weakly with the water molecules of the host lattice (5, 6).

The earlier dielectric studies of the water relaxation in clathrate hydrates were mainly confined to hydrates of rather large water-soluble ethers and ketones, viz. those of acetone (7); ethylene oxide (8); tetrahydrofuran, 2,5-dihydrofuran, propylene oxide, and trimethylene oxide (9); 1,3-dioxolane (10); dimethyl ether and cyclobutanone (11). In these hydrates the relaxation rates were found to be several orders of magnitude faster than in ice I and the activation energies only about half as great. Although the shapes of the dispersion loci appeared to be characteristic of the lattice structure for the structure II hydrates (9–11), the relaxation rates depended somewhat on the nature of the guest molecules. Except for the structure I hydrate of ethylene oxide (12), the smaller cages of all these hydrates are essentially unoccupied. Moreover, all of these hydrate formers are capable of relatively strong interaction, i.e. of hydrogen bonding, with water molecules. It is known from microwave absorption measurements (6) that in ethylene oxide and tetrahydrofuran hydrates the rotation of the guest molecules is only slightly hindered, but this does not exclude the possibility that a guest molecule may occasionally hydrogen bond to a lattice water molecule. Since these factors may well affect the details of the mechanism of relaxation of the water lattice, it is of considerable interest to examine the relaxation behavior of hydrates of small nonpolar molecules which fill both large and small cages almost quantitatively and which are incapable of hydrogen bonding to the water molecules of the lattice.

The results of a study of the temperature and pressure dependence of the dielectric properties of argon and nitrogen hydrates are reported here. Argon is the smallest molecule known to form a clathrate hydrate. Its hydrate is stable at 0 °C under argon pressures greater than 96 bars (13). Nitrogen hydrate is stable at 0 °C under pressures above 160 bars (13, 14). The decomposition pressures of both hydrates reach 1700 bars at 25 °C.

Experimental Methods

The cell (shown schematically in Fig. 1) consisted of a three-terminal stainless-steel coaxial electrode system mounted in a Teflon cylinder B which was contained by a brass sleeve. The bottom of B was attached to the lower pressure head by the binding post C, which was electrically connected to the outer (high-potential) electrode. The low-potential electrode A was guarded at the bottom. A brass ring D provided shielding between the binding posts C and E in the gas-filled region where their mutual capacitance would otherwise be variable. A small fixed capacitance resulted from interaction within the insulation between binding posts and mounting screws. This

[1]Issued as NRCC No. 9962.

and the cell constant were measured by calibration with air, cyclohexane, and conductivity water. The electrical connections, seals, and pressure vessel were as previously described (2).

Pressure was generated by a compressed-air-driven oil pump and transmitted to argon or nitrogen by a 3-kbar gas compressor. Pressures were read on a large calibrated 3-kbar Heise gauge. The pressure vessel containing the cell was immersed in an ethanol bath cooled to as low as −100 °C by a three-stage refrigeration unit designed and built by the Plant Engineering Division of NRCC. The bath temperature was regulated by adjustment of the flow rate of refrigerant through the cooling coils and by thermistor-controlled immersion heaters. Temperatures were measured by a calibrated copper–constantan thermocouple F (Fig. 1) inserted into the lower head of the pressure vessel to within 3″ of the center of the sample.

Capacitance and loss between 50 Hz and 500 kHz were measured by the earlier methods (15). For nitrogen hydrate measurements were extended to 0.05 Hz by use of a low-frequency bridge constructed according to a design of Professor R. H. Cole, to whom we are indebted.

The hydrates were grown in situ by subjecting freshly degassed conductivity water to gas pressures much above the hydrate decomposition pressure. Formation of hydrate, which was followed by changes in the dielectric properties of the sample, was very slow, presumably because of a hydrate crust formed at the water–gas interface. Repeated temperature and pressure cycling between about +10 and −40 °C and 1 and 3 kbar increased the formation rate, probably by cracking this crust. Even so, complete conversion to hydrate usually required from 3 to 5 weeks.

The problem of quantitative formation of clathrate hydrates of water-insoluble molecules, even with shaking, has long plagued attempts to define their compositions accurately. (See, for example, ref. 16 for a review of early disagreements in analyses, and ref. 13 for a recent unsuccessful attempt to directly determine the composition of methane hydrate.) For the present hydrates, the conductances measured at frequencies small in comparison with the frequency of maximum dielectric absorption were particularly sensitive to small quantities of water in the sample and served to monitor the disappearance of liquid water. Excess water in a sample of argon hydrate formed at 3 kbar led at low temperatures to a separate absorption region at higher frequencies whose amplitude diminished with conditioning and which was attributed to ice III.

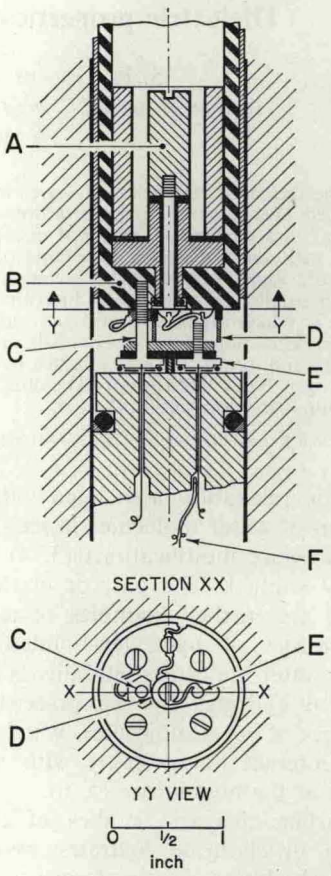

FIG. 1. Schematic of dielectric cell assembly.

Results

The Dispersion Loci

Typical experimental complex dielectric constant plots of argon and nitrogen hydrates are given in Figs. 2 and 3. In all some 50 such curves were obtained. The shapes conform quite closely to depressed circular arcs. The Cole–Cole α parameter increases greatly with decreasing temperature from values of about 0.1 at temperatures above 0 °C to 0.25 (for nitrogen hydrate) at −70 °C. The dispersion loci of nitrogen hydrate are somewhat broader than those of argon hydrate at the same temperature.

As with the hydrates previously studied (7, 9, 10) there are noticeable departures from arcs at low temperatures, especially at high frequencies where ε'' approaches the ε' axis more steeply than the circular arc. Departures of this kind also are observed on the low-frequency side of the absorption region when not obscured by the additional absorption associated with ionic conductance (see Fig. 3, upper locus).

In deriving dielectric parameters from the experimental data, we have taken the Cole–Cole representation (see eq. [1], p. 1676) to be adequate, except for ε_∞, which was obtained by extrapolation to the ε' axis of the high-frequency side of the experimental locus rather than from the best fit of a circular arc to the locus as a whole.

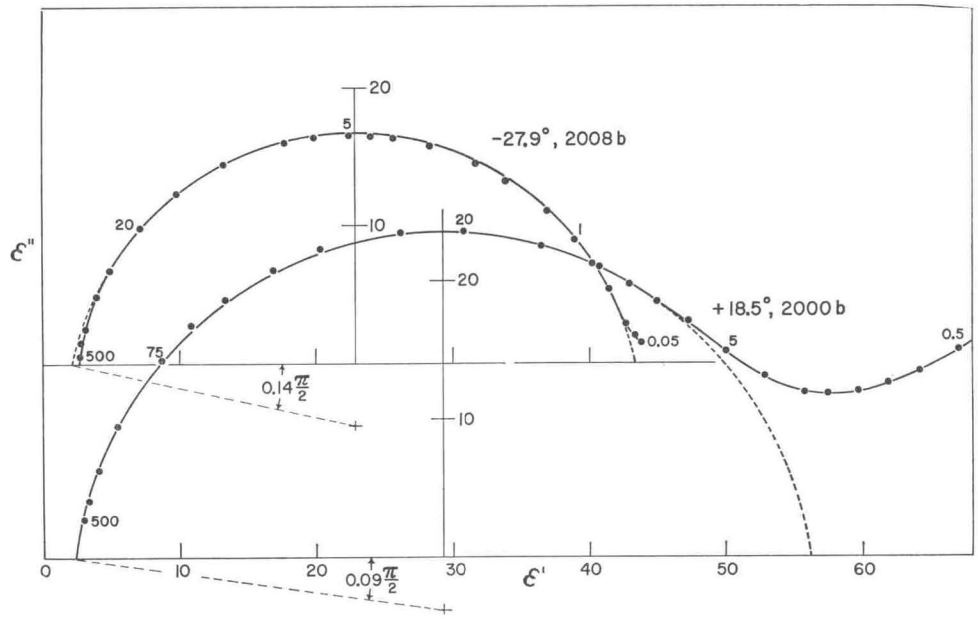

FIG. 2. Complex permittivity loci of argon hydrate. Numbers on loci are frequencies in kHz.

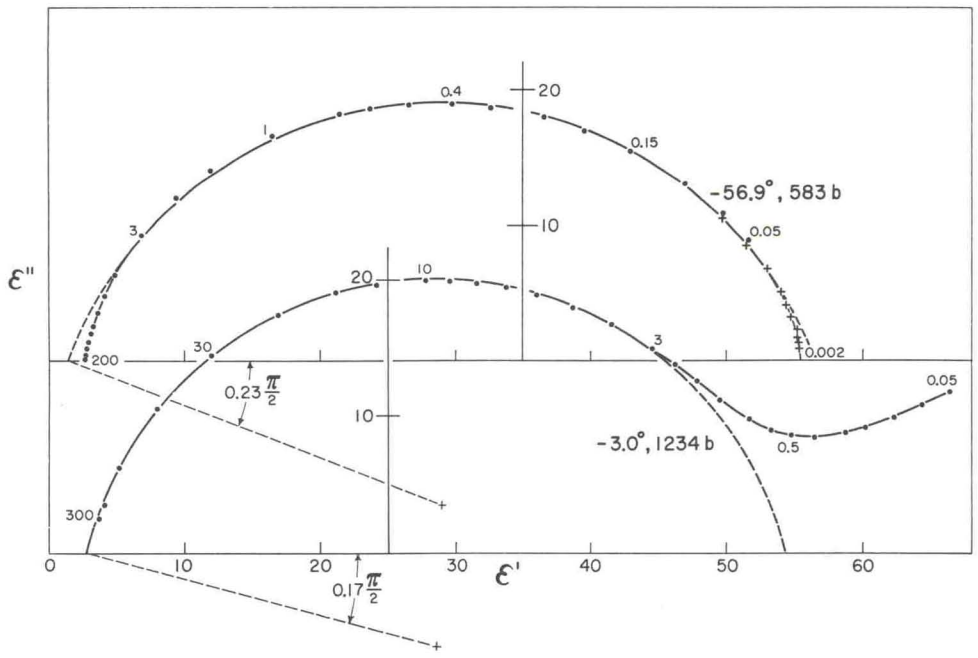

FIG. 3. Complex permittivity loci of nitrogen hydrate. Crosses refer to low-frequency bridge measurements.

TABLE I

Representative dielectric parameters

Sample	t (°C)	P/bar	ε_0(exp)	τ(exp)/μs	α	ε_0 (eq. [9])	τ/μs (eq. [8])	$10^3\,\delta$
				Argon hydrate				
1	18.5	2000	54.3	8.0	.08	53.7	8.0	0
1	18.8	2985	48.3	7.3	.08	54.2	8.3	3
1	9.2	2080	41.6	9.5	.09	55.4	13.0	9
2	3.9	2010	48.7	11.4	.12	56.4	13.5	4
1	−4.5	1990	33.9	11.8	.09	58.0	21.2	18
2	−13.3	2028	45.8	20.4	.12	59.8	27.6	8
2	−22.8	2013	43.4	27.0	.13	61.9	40.6	10
2	−28.1	2000	41.4	31.8	.14	63.2	52.0	13
				Nitrogen hydrate				
3	10.5	1795	~60	8.2	.11	55.0	8.2	0
2	3.0	1233	58	12.6	.14	56.1	12.6	0
1	−9.3	592	55.4	21.7	.17	58.2	23.0	1
1	−21.8	620	52.4	39.8	.20	60.9	48.1	3
2	−35.4	1235	64.6	161	.21	64.5	161	0
1	−45.6	1255	53.7	242	.20	67.2	319	5
3	−50.3	3	57.4	215	.22	67.7	317	3
3	−69.8	1	43.2	730	.26	73.8	1520	10
2	−70.8	808	67.6	1150	.23	74.8	1320	2

Some representative experimental values of static dielectric constant ε_0(exp), α, and relaxation time τ(exp) are given in Table I. Values of ε_∞ lay in the range 2.70 to 2.85.

At relatively high temperatures the measured static dielectric constants (e.g. 54 ± 2 for argon hydrate at 20 °C, 56 ± 2 for nitrogen hydrate at 0 °C) were quite reproducible and, despite the difference of lattice structure, similar to values (e.g. 57 ± 2 at 20 °C) estimated from earlier measurements of structure II hydrates of polar molecules (9, 10) with the dipolar contribution of the guest molecules subtracted. At lower temperatures, however, the apparent values of the static dielectric constant varied considerably from sample to sample and with sample history. They sometimes showed a decrease with decrease of temperature, especially marked for argon hydrate, rather than the increase expected. These effects undoubtedly arose from cracking or shrinkage of the samples away from the electrode surfaces. Such sample contraction affects not only the amplitude of the measured dispersion locus, but also its dependence on frequency. An analysis of contraction effects follows.

The Uniform Gap Model for Cole–Cole Behavior

The complex dielectric constant of the Cole–Cole locus is (17)

$$[1] \qquad \varepsilon^* = \varepsilon_\infty + \Delta\varepsilon[1 + (ix)^\beta]^{-1},$$

where $\Delta\varepsilon$ is $(\varepsilon_0 - \varepsilon_\infty)$, $x = \omega\tau$, τ is the relaxation time corresponding to $1/\omega$ at the frequency of maximum dielectric absorption, and $\beta = 1-\alpha$.

If the effect of sample shrinkage may be represented by a gap of uniform thickness a fraction δ of the interelectrode distance, in series with the sample, the measured complex dielectric constant is

$$[2] \qquad \varepsilon^*(\text{exp}) = k\varepsilon^*[\delta\varepsilon^* + (1 - \delta)k]^{-1},$$

where ε^* is the sample complex dielectric constant and k is the dielectric constant (assumed to have only a real component) of the medium which fills the gap. Substitution of [1] in [2] leads to

$$[3] \qquad \varepsilon^*(\text{exp}) = [k\varepsilon_0 + k\varepsilon_\infty(ix)^\beta] \times [b + a(ix)^\beta]^{-1},$$

in which $a = \delta\varepsilon_\infty + (1 - \delta)k$ and $b = \delta\varepsilon_0 + (1 - \delta)k$. At the low- and high-frequency limits eq. [3] reduces to

$$[4] \qquad \varepsilon_0(\text{exp}) = k\varepsilon_0/b \text{ and } \varepsilon_\infty(\text{exp}) = k\varepsilon_\infty/a.$$

Substitution for ε_0 and ε_∞ in eq. [3] gives

$$[5] \qquad \varepsilon^*(\text{exp}) = \varepsilon_\infty(\text{exp}) + \Delta\varepsilon(\text{exp})[1 + (a/b)(ix)^\beta]^{-1}$$

in which $\Delta\varepsilon(\text{exp}) = \varepsilon_0(\text{exp}) - \varepsilon_\infty(\text{exp})$. Equation [5] has the same form as the Cole–Cole eq. [1] and describes a locus of the same shape. However, $x^\beta = \omega^\beta\tau^\beta$ has been replaced by

TABLE II

Effect of the gap corrections for nitrogen hydrate

t (°C)	P/bar	ε_0(exp)	τ(exp)/μs	α	ε_0 (eq. [9])	τ/μs (eq. [8])	$10^3\,\delta$
−3.03	1234	54.3	16.8	0.17	57.3	17.9	1.3
−3.24	1888	48.4	15.6	0.17	57.6	19.2	4.7
−3.26	601	52.2	15.9	0.17	57.0	17.7	2.0
−3.32	1233	47.1	14.5	0.17	57.3	18.3	5.1

$(a/b)x^\beta = \omega^\beta(a/b)\tau^\beta$, that is, the apparent relaxation time is now

$$[6] \qquad \tau(\text{exp}) = (a/b)^{1/\beta}\tau.$$

To the extent that the observed dispersion loci are Cole–Cole arcs the adequacy of this model may be tested by the consistency of the values of τ derived from experimental relaxation times by use of eq. [6]. For this purpose the proper values of ε_0 and ε_∞ are required. A knowledge of k is not explicitly required for eq. [6], but is necessary for an estimation of the effective gap thickness

$$[7]^2 \qquad \delta = k\left[\frac{\epsilon_0}{\epsilon_0(\text{exp})} - 1\right](\epsilon_0 - k)^{-1}.$$

If δ and ε_∞ are small, and $\varepsilon_0 \gg \varepsilon_\infty$, little error is introduced by putting $a/b = \varepsilon_0(\text{exp})/\varepsilon_0$, whence

$$[8] \qquad \tau = [\varepsilon_0/\varepsilon_0(\text{exp})]^{1/(1-\alpha)}\tau(\text{exp}).$$

Application of the Gap Model to the Data

For application of eq. [8], ε_0 as a function of temperature and pressure is required. For argon and nitrogen hydrates we take

$$[9] \qquad \varepsilon_0 = (4.0 + 14200/T)(1 + 0.010P),$$

where P is the pressure in kbar. This equation fits the experimental values of ε_0 (± 2) at high temperatures, when the gaps are inappreciable, and allows for variations of ε_0 with temperature and pressure similar to those of the other forms of ice (1–3).

Values of ε_0 from [9] and of τ from [8] are included in Table I, along with the estimates of the relative gap thickness δ from [7]. Values of k were crudely evaluated by extrapolating to lower temperatures the dielectric constants of gaseous argon and nitrogen measured under pressure (18, 19). Values of δ did not exceed 0.015 for nitrogen hydrate and 0.018 for argon hydrate.

The gap correction reduces considerably the variability of the original relaxation time τ(exp). The data in Table II for sample 2 of nitrogen hydrate at −3 °C illustrate this. The relaxation times for the two sets of measurements at 1230 bar are brought into close agreement and the τ's now clearly increase with increasing pressure as they do for other ices (2–4). Figure 4 shows the general improvement in consistency which results.

The series-gap treatment does not reduce the scatter of the relaxation times, particularly between different samples, to the level of uncertainty (ca. 1%) with which τ may be measured in the absence of gaps. Some of the residual scatter suggests overcorrection for the larger gaps. This may arise because the real static dielectric constants are somewhat less than those given by eq. [9] or the gaps are not of uniform thickness. However, certain consistent differences between results for different samples suggest some variation of the relaxation behavior with the conditions of preparation and history of the sample. Thus initial measurements on sample 3 of nitrogen hydrate at a number of temperatures (not shown in Fig. 4) yielded smaller α's and τ's than those previously measured. These anomalies, which do not seem attributable to the presence of ice, disappeared after several days of conditioning.

Discussion

High-Frequency Dielectric Constants

Values of ε_∞ for both argon and nitrogen hydrate (2.85 $\pm$ 0.05 at −30 °C after small gap

[2]Strictly, δ is the ratio of gap thickness to electrode separation only for parallel plate electrodes. For cylindrical coaxial electrodes of radii u and v, δ in the above equations is replaced by $\Delta r/[r \ln (v/u)]$, where r is the radial position of a small gap of uniform thickness Δr. In the likely event that contraction occurs by shrinkage away from the outer electrode, δ is replaced, for the actual electrodes used, by $0.78\delta'$, where $\delta' = \Delta r/(v-u)$.

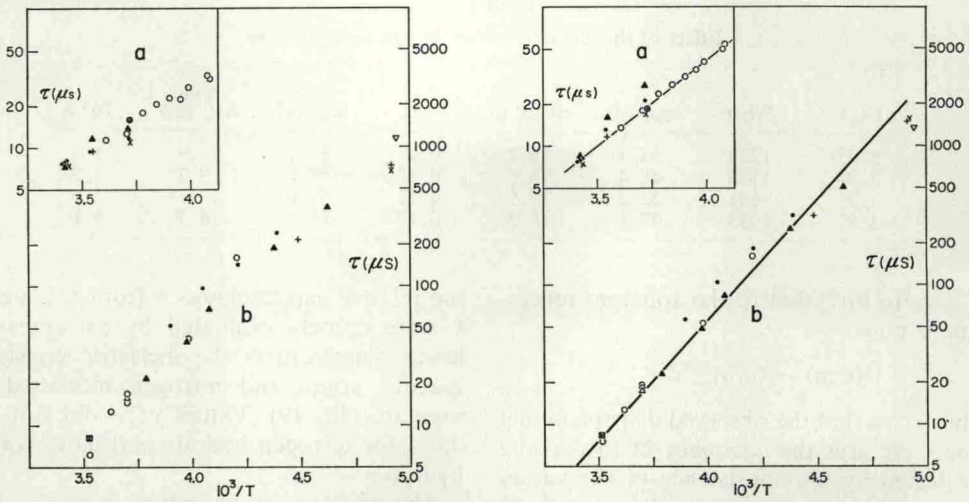

FIG. 4. Experimental (left) and gap-corrected (right) relaxation times at various pressures. (*a*) Argon hydrate. Sample 1: ⊕, 300; +, 800; ×, 1100; ●, 2000; ▲, 3000 bar. Sample 2: ○, 2000 bar. (*b*) Nitrogen hydrate. Sample 1: ▲, 600; ●, 1240 bar. Sample 2: △, 620; ▽, 810; ○, 1240 bar. Sample 3: +, 1; ×, 310;□, 1800 bar.

corrections) are similar to that of ice (3.1), in contrast to the much higher values found for the hydrates of dipolar molecules, to which the reorientation of the guest molecules makes a large contribution (6, 9, 10).

For a solution of argon or nitrogen in the structure I hydrate lattice the Onsager equation may be written (20)

$$[10]\quad \frac{(\epsilon_\infty - 1)(2\epsilon_\infty + 1)}{3\epsilon_\infty} = \frac{4\pi N_0\alpha_0}{1 - f_0\alpha_0} + \frac{4\pi N_1\alpha_1}{1 - f_1\alpha_1},$$

where N is the number density of molecules, α is the molecular polarizability, $f\alpha$ allows for the reaction field, and the subscripts 0 and 1 refer respectively to water and argon or nitrogen. The empty lattice contribution cannot be evaluated in terms of the polarizability of the isolated water molecule since lattice vibrations make important contributions. Instead, we take

$$[11]\quad \frac{4\pi N_0\alpha_0}{1 - f_0\alpha_0} \simeq \left[\frac{(\epsilon_\infty - 1)(2\epsilon_\infty + 1)}{3\epsilon_\infty N_0}\right]_{\text{ice I}} N_0,$$

in which ϵ_∞ and N_0 in the square brackets refer to ice I. Equation [11] assumes a contribution, per water molecule, of the empty hydrate lattice equal to that of ice and leads to a value of ϵ_∞ of 2.78 for the empty lattice if the unit cell dimension is 12.05 Å. Addition of the contribution of the encaged molecules gives $\epsilon_\infty = 2.90$ for argon hydrate and $\epsilon_\infty = 2.91$ for nitrogen hydrate if all the cages are occupied.

Thus eq. [11] appears to provide a good approximation to the effective polarizability of the water lattice in these hydrates. As in ice, ϵ_∞ is considerably greater than n_D^2 which is ~ 1.72 for both hydrates and ice. It is probable that the lattice vibrations are similar, especially the translational modes which are associated with the optical density maximum in ice at 229.2 cm^{-1} at 100 °K (21). Even after correction for gaps, values of ϵ_∞ for nitrogen hydrate decrease slightly with decrease of temperature, despite the increase of density. This decrease amounts to 0.08 ± 0.04 between −30 and −94 °C and probably arises from a general shift toward higher frequencies of the lattice modes.

Static Dielectric Constants

Since encaged argon and nitrogen molecules contribute only about 0.1 to the dielectric constants, the static dielectric constants are essentially those of the ice-like lattice. Substitution of $\epsilon_0 = 56$ at 0 °C into the Kirkwood equation in the form

$$[12]\quad \epsilon_0 - \epsilon_\infty = 2\pi N_0[(n^2 + 2)/3]^2 g\mu^2/kT,$$

with $n^2 = 1.60$ (from the Lorentz–Lorenz equation and $n^2 = 1.72$ for ice) and $\mu = 1.84$ D,

TABLE III

Relaxation times and activation parameters for structure I hydrates and ices I and III at 0 °C

	P/bar	τ/μs	E_A (kcal mole^{-1})	$\Delta S^{\ddagger}$ (cal deg^{-1} mole^{-1})	$\Delta V^{\ddagger}$ (cm^3 mole^{-1})	Reference
Argon hydrate	2000	16	5.7	−17.5	3	This work
Nitrogen hydrate	1200	15	7.9	− 9.4	2	This work
Ethylene oxide hydrate	1	0.027	6.7	− 1.2		8
Trimethylene oxide hydrate*	1	0.005	5.8	− 1.3		9
Ice I	1	21.5	13.25	+ 9.5	2.9 (−23 °C)	1, 2
Ice III†	3000	0.19	11.6	+13.0	4.5 (−30 °C)	3

*Extrapolated from data below −74 °C.
†Extrapolated from data below −22 °C.

gives a g value of 2.5. This is significantly smaller than the value of 3.3 for ice I, but is comparable to the value of 2.7 found for ice III (3) and for structure II hydrates (9). Clearly again the hydrogen bonding imposes a considerable local correlation between the directions of the dipole moments of water molecules.

Relaxation Times

Reorientation of the water molecules in argon and nitrogen hydrates is remarkably slow in comparison with their reorientation in the clathrate hydrates previously studied. The relaxation times at 0° C (Table III) are larger by several orders of magnitude than those of the isostructural hydrates of ethylene oxide (8) and trimethylene oxide, the latter extrapolated from results at much lower temperatures (9).[3] The structure II hydrates of several ethers and ketones (7, 9–11), have relaxation times of about 0.1 μs at 0 °C.

At relatively high temperatures, argon and nitrogen hydrates relax as slowly as ice I, the slowest of the disordered ices to relax. The relaxation times depend much less on temperature, however, and the activation energies (Table III) are similar to those of other hydrates.

The activation volumes (2 or 3 cm^3 mole^{-1}) are indistinguishable from the activation volume of ice I. Because of small differences between samples, and the small effect of pressure on the relaxation times, activation volumes were derived only from measurements on the same sample. They almost certainly refer to hydrates of constant composition, rather than to hydrates whose compositions attain new equilibrium values in response to a change of pressure.

Shape of the Dispersion Curves

The shapes of the dispersion loci of structure II hydrates and their change with temperature appear to be characteristic of the crystal structure (9–11). This is not the case for the four structure I hydrates for which information is available if the shapes are compared at the same temperatures. Values of α of about 0.1 are found above 0 °C for argon and nitrogen hydrates, at −80 °C for ethylene oxide hydrate, and at −110 °C for trimethylene oxide hydrate, at which temperatures the relaxation times of all these hydrates are similar. However, if the width of the dispersion is entirely dictated by the degree of non-equivalence of water molecule sites and hydrogen bonds in the lattice, identical structures should lead to identical α's at the same temperature. The size of the unit cell is known to vary slightly for different encaged molecules (23, 24). The extent to which the positions of the water molecules vary within the unit cell is unknown, but is likely to be too small to markedly affect the value of α. The relatively broad loci shown by argon and nitrogen hydrates are probably partly due to factors other than non-equivalence of the hydrogen bonds (see next section).

Mechanism of Relaxation

There are several suggestive regularities in the activation parameters for relaxation of the various phases of "ice" listed in Table III of this paper and in Table III of the following paper (25). The Arrhenius activation energies fall into two groups, with values in the ranges 5.7 to 8.7 (average about 7) and 11.0 to 13.3 kcal mole^{-1}, respectively. The group with high

[3] In addition to a hydrate of structure II, trimethylene oxide forms a second hydrate (9) which Calvert's X-ray diffraction studies (22) have now confirmed to be structure I.

activation energies is also characterized by relatively high positive entropies of activation, 9 to 13 cal deg^{-1} $mole^{-1}$. The group with low activation energies may be subdivided into the ether and ketone hydrates, with entropies of activation close to zero, and argon and nitrogen hydrates, with large negative activation entropies.

According to the Bjerrum model of relaxation in ice (26), reorientation of water molecules occurs by the diffusion of D and L defects, that is, of O - - - O "bonds" which have either two hydrogen atoms or none near them. In pure ice I these defects are formed by thermal excitation of normal hydrogen bonds N

$$2N \rightleftharpoons D + L,$$

for which an enthalpy and entropy of formation of 15.7 kcal $mole^{-1}$ and −4.2 cal deg^{-1} $mole^{-1}$ may be estimated (27). The activation enthalpy and entropy for the diffusion of the defects are then 4.9 kcal $mole^{-1}$ and 11.6 cal deg^{-1} $mole^{-1}$, where the dielectric Arrhenius energy (Table III) has been converted to an enthalpy of activation at 0 °C.

Ices III, V, VI, and VII have (high) energies and entropies of activation like ice I and appear to relax by essentially the same mechanism (2–4). The hydrogen bonding between the water molecules of the clathrate hydrates of types I and II approaches more closely that in ice I than does the hydrogen bonding in the high-pressure ices. All water molecules are four-coordinated and in the structure I ethylene oxide hydrate at −25 °C (12) for example the average nearest-neighbor O - - - O distance is 2.79 Å and the average departure of the O - - - O - - - O angles from tetrahedral is only 3.7°. It is therefore likely that the clathrate hydrates also relax by diffusion of orientational defects, although the details of the Bjerrum mechanism must be modified to account for the appreciable lowering of the energies and entropies of activation.

The similarity of the activation parameters shown by the ices proper, despite their diverse structures, suggests that the thermodynamic parameters for the formation and diffusion of the defects responsible for relaxation are similar in these phases. We neglect small differences and assume, because of the structural similarities, that the parameters for the *intrinsic* formation and diffusion of the defects are the same in the clathrate hydrates as in ice I.

The fact that the ether and ketone hydrates relax faster than ice suggests that, in addition to intrinsic defects, defects are introduced into the lattice of these clathrate hydrates by interaction of the water with guest molecules. This is further indicated by the existence of differences between the relaxation rates of the isostructural hydrates of different ethers and ketones. The most probable form of this interaction with a guest molecule M produces something resembling an L defect

$$M + N \rightleftharpoons M - - - H—O + L,$$

where N stands for a normal hydrogen bond. The equilibrium constant is

$$K = \frac{c_N}{c_M}\alpha^2,$$

where α is the fraction of normal bonds converted to defects. The ratio c_N/c_M of the concentration of normal bonds to the concentration of guest molecules varies from 11.5 for structure I hydrates with all cages occupied to 34 for structure II hydrates. From the representative Arrhenius energy and entropy of activation of 7 kcal $mole^{-1}$ and 0 cal deg^{-1} $mole^{-1}$ for these hydrates, the energy and entropy of formation of defects are about 3 kcal $mole^{-1}$ and −23 cal deg^{-1} $mole^{-1}$, K is about 2×10^{-8} at −10° C, and α is about 3×10^{-5}. In ice I the fraction α of defect to normal bonds is much less, about 10^{-7} at −10 °C. The energy of defect formation is reasonable: the geometry is less favorable than for hydrogen bonding within the lattice and very roughly half the energy of a hydrogen bond has to be paid. The entropy of formation is also reasonable since a large part of the translational and rotational entropy of the guest is lost when it is tied at one point.

It is not possible to explain the large negative apparent entropies of activation of argon and nitrogen hydrates by such an interaction between the encaged and host molecules as has been suggested above for the ether and ketone hydrates. The most likely explanation is that argon or nitrogen molecules occasionally substitute for water molecules as "impurities" in the lattice during the formation of the hydrate at about 2 kbar gas pressure. The van der Waals radii (1.90 Å for argon and 2.05 Å for nitrogen)

are somewhat larger than the effective radius of the water molecule (1.40 Å) and some distortion of the local structure would accompany substitution. Each substitution would tend to inject up to 2 D defects into the lattice. Such a mechanism of defect formation would account for the unexpected breadth of the dispersion loci and for its large temperature dependence (last section), as well as for the differences between the activation energies and entropies of the two hydrates. It is consistent with the volumes of activation.

It is instructive to compare the effect of impurities, including air, on the relaxation of ice I. For "slightly impure" ice, $\log \tau$ vs. $1/T$ plots show curvature toward decreasing slopes at low temperatures in both dielectric (11) and spin-lattice (28, 29) relaxation time measurements. In the dielectric case, additional absorption appears at relatively high frequencies to broaden the dispersion loci. Impurities clearly act as sources of orientational defects, the effect of which is not purely local since the whole relaxation spectrum is shifted to higher frequencies. At low enough temperatures defects so originating outnumber those arising intrinsically in ice and the activation energy and entropy become appreciably smaller.

Since argon and nitrogen hydrates have nearly the same relaxation times as ice I at 0 °C, about the same fraction of normal bonds is converted to defects, i.e. about 3×10^{-7}. The impurity-induced defects must be more numerous than the intrinsic defects or the activation energy would be temperature dependent.

This semiquantitative discussion has neglected the differences between the different "ice" structures and between the D and L defects, and is by no means complete. It does, however, serve to explain in a general way the dielectric behavior.

The lattice impurity mechanism suggested for argon and nitrogen hydrates would not be expected to determine the rate of defect formation in the hydrates of much larger molecules which would substitute with more difficulty. Relaxation in SF_6 hydrate is considered in the following paper (25).

Acknowledgments

We are indebted to R. E. Hawkins for help in the construction of the cell and to A. Lavergne for installation and maintenance of the high-pressure equipment.

1. R. P. Auty and R. H. Cole. J. Chem. Phys. **20**, 1309 (1952).
2. R. K. Chan, D. W. Davidson, and E. Whalley. J. Chem. Phys. **43**, 2376 (1965).
3. G. J. Wilson, R. K. Chan, D. W. Davidson, and E. Whalley. J. Chem. Phys. **43**, 2384 (1965).
4. E. Whalley, D. W. Davidson, and J. B. R. Heath. J. Chem. Phys. **45**, 3976 (1966).
5. G. A. Jeffrey and R. K. McMullan. *In* Progress in inorganic chemistry .Vol. 8. *Edited by* F. A. Cotton. Interscience Publishers, New York. 1967.
6. D. W. Davidson, M. M. Davies, and K. Williams. J. Chem. Phys. **40**, 3449 (1964).
7. G. J. Wilson and D. W. Davidson. Can. J. Chem. **41**, 264 (1963).
8. D. W. Davidson and G. J. Wilson. Can. J. Chem. **41**, 1424 (1963).
9. R. E. Hawkins and D. W. Davidson. J. Phys. Chem. **70**, 1889 (1966).
10. A. Venkateswaran, J. R. Easterfield, and D. W. Davidson. Can. J. Chem. **45**, 884 (1967).
11. D. W. Davidson. Unpublished work.
12. R. K. McMullan and G. A. Jeffrey. J. Chem. Phys. **42**, 2725 (1965).
13. D. R. Marshall, S. Saito, and R. Kobayashi. A.I.Ch.E. J. **10**, 202, 723 (1964).
14. A. van Cleeff and G. A. M. Diepen. Rec. Trav. Chim. **79**, 582 (1960); **84**, 1085 (1965).
15. A. D. Potts and D. W. Davidson. J. Phys. Chem. **69**, 996 (1965).
16. W. Schroeder. Ahren's Sammlung Chemischer und Chemisch-technischer Vortrage, **29**, 1 (1926).
17. K. S. Cole and R. H. Cole. J. Chem. Phys. **9**, 341 (1941).
18. A. Michels, C. A. ten Seldam, and S. D. J. Overdijk. Physica, **17**, 781 (1951).
19. A. Michels, A. Jaspers, and P. Sanders. Physica, **1**, 627 (1934).
20. C. J. F. Böttcher. Theory of electric polarization. Elsevier Publishing Co., New York. 1952. p. 318.
21. J. E. Bertie and E. Whalley. J. Chem. Phys. **46**, 1271 (1967).
22. L. D. Calvert. Private communication.
23. M. von Stackelberg and W. Jahns. Z. Elektrochem. **58**, 162 (1954).
24. D. F. Sargent and L. D. Calvert. J. Phys. Chem. **70**, 2689 (1966).
25. Y. A. Majid, S. K. Garg, and D. W. Davidson. Can. J. Chem. This issue.
26. N. Bjerrum. Kgl. Danske Videnskab. Selskab Mat. Fys. Medd. **27**, 3 (1951).
27. H. Gränicher. Physik Kondensierten Materie, **1**, 1 (1963).
28. K. Kume. J. Phys. Soc. Japan, **15**, 1493 (1960).
29. D. E. Barnaal. Ph.D. Dissertation, University of Minnesota, Minneapolis, Minnesota. 1965. University Microfilms 65-7867, Ann Arbor, Mich.